

Strong coupling, energy splitting, and level crossings: A classical perspective

Lukas Novotny^{a)}

Institute of Optics, University of Rochester, Rochester, New York 14627

(Received 20 January 2010; accepted 6 July 2010)

Strongly interacting quantum systems are at the heart of many physical processes, ranging from photosynthesis to quantum information. We demonstrate that many characteristic features of strongly coupled systems can be derived classically for a simple coupled harmonic oscillator. This model system is used to derive frequency splittings and to analyze adiabatic and diabatic transitions between the coupled states. A classical analog of the Landau–Zener formula is derived. The classical analysis is intuitive and well suited for introducing students to the basic concepts of strongly interacting systems. © 2010 American Association of Physics Teachers.

[DOI: 10.1119/1.3471177]

I. INTRODUCTION

The interaction between quantum systems is commonly studied in the weak coupling and the strong coupling limits. Weak coupling can be treated within perturbation theory, and various classical analogs have been developed.^{1–3} Examples of the effects of weak coupling are changes in atomic decay rates⁴ (Purcell effect) and Förster energy transfer⁵ between a donor and acceptor atom or molecule. Förster energy transfer assumes that the transfer rate from donor to acceptor is smaller than the relaxation rate of the acceptor. This assumption ensures that once the energy is transferred to the acceptor, there is little chance of a back transfer to the donor. Once the interaction energy becomes sufficiently large, and a back transfer to the donor becomes possible, the system is in the strong coupling regime. In this limit, it is no longer possible to distinguish between donor and acceptor. Instead, the excitation becomes delocalized, and we must view the pair as one system. A characteristic feature of the strong coupling regime is energy level splitting, a property that can be well understood from a classical perspective.

Coupled harmonic oscillators are an intuitive and popular model for many phenomena, including electromagnetically induced transparency,⁶ level repulsion,⁷ nonadiabatic processes,⁸ and rapid adiabatic passage.⁹ In this article, we use a coupled oscillator model as a canonical example for strong coupling and derive frequency splittings and conditions for adiabatic and diabatic transitions.

II. COUPLED OSCILLATORS

In the absence of coupling ($\kappa=0$), the two oscillators shown in Fig. 1 have eigenfrequencies $\omega_A^0 = \sqrt{k_A/m_A}$ and $\omega_B^0 = \sqrt{k_B/m_B}$, respectively. In the presence of coupling ($\kappa \neq 0$), the equations of motion become

$$m_A \ddot{x}_A + k_A x_A + \kappa(x_A - x_B) = 0 \quad (1a)$$

$$m_B \ddot{x}_B + k_B x_B - \kappa(x_A - x_B) = 0. \quad (1b)$$

We seek solutions of the form $x_i(t) = x_i^0 \exp[-i\omega_{\pm}t]$, where ω_{\pm} are the new eigenfrequencies. We insert this ansatz into Eqs. (1) and obtain two coupled linear equations for x_A^0 and x_B^0 , which can be written in matrix form as $\vec{M}[x_A^0, x_B^0]^T = 0$. Nontrivial solutions for this homogeneous system of equa-

tions exist only if $\det[\vec{M}] = 0$. The resulting characteristic equation yields

$$\omega_{\pm}^2 = \frac{1}{2}[\omega_A^2 + \omega_B^2 \pm \sqrt{(\omega_A^2 - \omega_B^2)^2 + 4\Gamma^2 \omega_A \omega_B}], \quad (2)$$

where $\omega_A = \sqrt{(k_A + \kappa)/m_A}$, $\omega_B = \sqrt{(k_B + \kappa)/m_B}$, and

$$\Gamma = \frac{\sqrt{\kappa/m_A} \sqrt{\kappa/m_B}}{\sqrt{\omega_A \omega_B}}. \quad (3)$$

In analogy to the dressed atom picture,¹⁰ the eigenfrequencies ω_{\pm} can be associated with dressed states, that is, the oscillator frequencies of systems A and B in the presence of mutual coupling.

To illustrate the solutions given by Eq. (2) we set $k_A = k_o$, $k_B = k_o + \Delta k$, and $m_A = m_B = m_o$. Figure 2(a) shows the frequencies of the two oscillators in the absence of coupling ($\kappa = 0$). As Δk is increased from $-k_o$ to k_o , the frequency of oscillator B increases from zero to $\sqrt{2}\omega_o$, while the frequency of oscillator A stays constant. The two curves intersect at $\Delta k = 0$. Once coupling is introduced, the two curves no longer intersect. Instead, as shown in Fig. 2(b), there is a characteristic anticrossing with a frequency splitting of

$$|\omega_+ - \omega_-| = \Gamma. \quad (4)$$

Anticrossing is a characteristic fingerprint of strong coupling. Because $\Gamma \propto \kappa$, the splitting increases with coupling strength.

Note that we have ignored damping in the analysis of the coupled oscillators. Damping can be readily introduced by adding the frictional terms $\gamma_A \dot{x}_A$ and $\gamma_B \dot{x}_B$ to Eqs. (1). The introduction of damping gives rise to complex frequency ei-

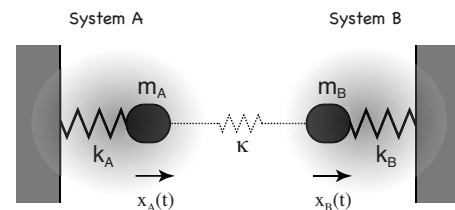


Fig. 1. Strong coupling regime illustrated by mechanical oscillators. The coupling κ of the two oscillators (mass m_i and spring constant k_i) leads to a shift of the eigenfrequencies and a characteristic frequency splitting.

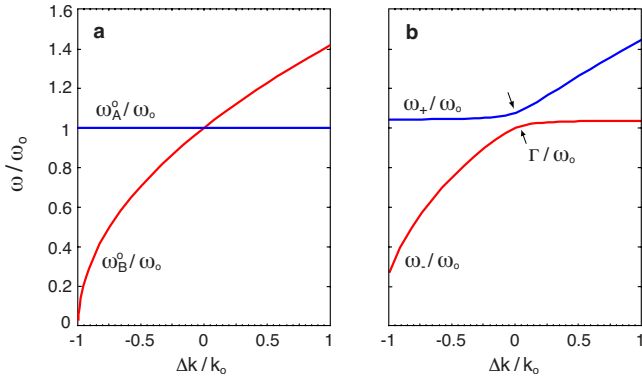


Fig. 2. (a) Eigenfrequencies of two uncoupled oscillators ($\kappa=0$) with equal mass and spring constants k_o and $k_o+\Delta k$. (b) Frequency anticrossing due to coupling of strength $\kappa=0.08k_o$. The frequency splitting $[\omega_+-\omega_-]$ scales linearly with the coupling strength κ .

genvalues, the imaginary part of which represents the linewidths. The latter gives rise to a “smearing out” of the curves shown in Fig. 2, and for very strong damping, it is no longer possible to discern the frequency splitting $[\omega_+-\omega_-]$. Therefore, to observe strong coupling, the frequency splitting needs to be larger than the sum of the linewidths,

$$\frac{\Gamma}{\gamma_A/m_A + \gamma_B/m_B} > 1. \quad (5)$$

In other words, the dissipation in each system needs to be smaller than the coupling strength.

Coupled mechanical oscillators are a generic model system for many physical systems, including atoms in external fields,¹¹ coupled quantum dots,¹² and cavity optomechanics.¹³ Although our analysis is purely classical, a quantum mechanical analysis yields the same result for the frequency splitting shown in Eq. (2).¹⁴ The coupling between energy states gives rise to avoided level crossings. The coupled oscillator picture can be readily extended by external forces $F_A(t)$ and $F_B(t)$ acting on the masses m_A and m_B to account for externally driven systems, as in the case of electromagnetically induced transparency.⁶

III. ADIABATIC AND DIABATIC TRANSITIONS

We now investigate what happens if one of the oscillator parameters changes as a function of time. For example, to determine the curves shown in Fig. 2, we need to tune Δk from an initial value of $-k_o$ to a final value k_o . Thus, Δk becomes a function of time, a fact that we have ignored in the analysis in Sec. II. We assumed that Δk is tuned so slowly that for every measurement window Δt the system parameters can be regarded as constant. Thus, if we initially have $\Delta k=-k_o$, the coupled system oscillates at frequency ω_- (bottom curve in Fig. 2(b)), and the system will follow the same curve as we slowly increase Δk . We can fine tune the oscillation frequency by adjusting Δk . The same applies if we initially start with frequency ω_+ [top curve in Fig. 2(b)]. In both cases the anticrossing region is passed by staying on the same branch. This scenario is referred to as an *adiabatic transition* and is illustrated in Fig. 3(a).

In the adiabatic limit, it is possible to transfer the energy from one oscillator to the other by slowly tuning the coupled system through resonance. To see this effect, we introduce normal coordinates (x_+, x_-) defined by

$$x_A(t) = x_+(t)\sin \beta + x_-(t)\cos \beta, \quad (6a)$$

$$x_B(t) = x_+(t)\cos \beta - x_-(t)\sin \beta, \quad (6b)$$

where β is determined by $\tan \beta = (\omega_B^2 - \omega_+^2) / (\kappa / m_B) = -(\omega_A^2 - \omega_-^2) / (\kappa / m_B)$. We substitute these expressions for x_A and x_B into Eqs. (1) and obtain

$$\ddot{x}_+(t) + \omega_+^2 x_+(t) = 0, \quad (7a)$$

$$\ddot{x}_-(t) + \omega_-^2 x_-(t) = 0, \quad (7b)$$

which represent two independent harmonic oscillators oscillating at the eigenfrequencies ω_{\pm} defined by Eq. (2). In other words, there are two sets of coordinates, x_+ and x_- , which oscillate independently from each other.

Now, imagine that Δk is slowly tuned in time from the initial value $\Delta k=-k_o$ through resonance to a value of $\Delta k=k_o$. According to Fig. 2, at the initial time we have $(\omega_A - \omega_-) \gg \Gamma$ and therefore $\beta \sim -\pi/2$. If we use this value in Eqs. (6) and assume that initially only oscillator A is active, we find that all the energy is associated with normal mode

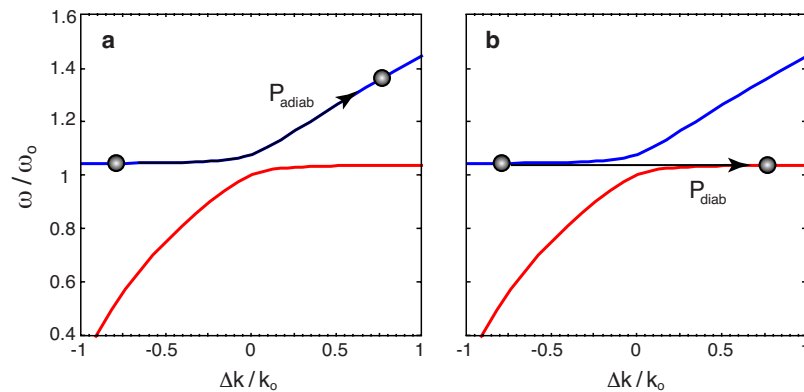


Fig. 3. Adiabatic and diabatic transitions caused by a time-varying Δk . (a) In the adiabatic case, the dynamics of the system is not affected by the time dependence of Δk , and the system evolves along the eigenmodes ω_{\pm} . (b) In the diabatic case, the time dependence of Δk gives rise to “level crossing,” a transition from one eigenmode to the other.

x_+ , that is, $x_- = 0$. Once Δk is tuned past resonance to k_o , we have $(\omega_A - \omega_-) \ll \Gamma$ and $\beta \approx 0$. According to Eqs. (6), the energy of mode x_+ now coincides with oscillator B , and hence the energy is transferred from oscillator A to oscillator B as the system is slowly tuned through resonance. If Δk changes in time, then k_B , ω_B , and the eigenfrequencies ω_{\pm} become time-dependent. If we assume a slowly varying $\omega_{\pm}(t)$ in Eqs. (7), we find

$$x_{\pm}(t) = x_{\pm}(t_i) \operatorname{Re} \left\{ \exp \left[i \int_{t_i}^t \omega_{\pm}(t') dt' \right] \right\}, \quad (8)$$

where we used the ansatz $x_{\pm}(t) = x_{\pm}(t_i) \exp[if(t)]$ and $[d^2f/dt^2] \ll [df/dt]^2$. Equation (8) describes the *adiabatic* evolution of the normal modes.

We now analyze what happens if we change Δk more rapidly. We use the ansatz

$$x_A(t) = x_o c_A(t) \exp[i\omega_A t], \quad x_B(t) = x_o c_B(t) \exp[i\omega_A t] \quad (9)$$

and assume that initially only oscillator A is active, that is, $c_B(-\infty) = 0$. The amplitude x_o is a normalization constant that ensures that $|c_A|^2 + |c_B|^2 = 1$. We substitute these expressions for x_A and x_B into Eqs. (1) and obtain the following coupled differential equations for c_A and c_B :

$$\ddot{c}_A + 2i\omega_A \dot{c}_A = (\kappa/m_A) c_B, \quad (10a)$$

$$\ddot{c}_B + 2i\omega_A \dot{c}_B + [\omega_B^2(t) - \omega_A^2] c_B = (\kappa/m_B) c_A, \quad (10b)$$

where we emphasized the time dependence of ω_B . For weak coupling between the two oscillators, the amplitudes $c_A(t)$ and $c_B(t)$ in Eq. (9) vary much slower in time than the oscillatory term $\exp[i\omega_A t]$. Therefore, $\ddot{c}_A \ll i\omega_A \dot{c}_A$ and $\ddot{c}_B \ll i\omega_A \dot{c}_B$, which allows us to drop the second-order derivatives in Eqs. (10) to obtain

$$2i\omega_A \dot{c}_A = (\kappa/m_A) c_B, \quad (11a)$$

$$2i\omega_A \dot{c}_B + [\omega_B^2(t) - \omega_A^2] c_B = (\kappa/m_B) c_A. \quad (11b)$$

From Eq. (11a), we find c_B and \dot{c}_B (by taking a derivative) and substitute the results into Eq. (11b) to find, after some algebra,

$$\ddot{c}_A - i\dot{c}_A \left[\frac{\omega_B^2(t) - \omega_A^2}{2\omega_A} \right] + c_A \frac{\kappa^2/[m_A m_B]}{4\omega_A^2} = 0. \quad (12)$$

The time dependence of ω_B makes Eq. (12) nonlinear. During the time interval of interest, close to the anticrossing region, $\omega_B(t) \approx \omega_A$, and hence $[\omega_B(t)^2 - \omega_A^2]/[2\omega_A] \approx [\omega_B(t) - \omega_A]$. For the same reason, we can set $\Gamma^2 \approx \kappa^2/[m_A m_B \omega_A^2]$ [see Eq. (3)]. Finally, we assume that near the anticrossing region, the frequency difference of oscillators A and B changes linearly in time, that is,

$$[\omega_B(t) - \omega_A] = \alpha t. \quad (13)$$

According to Eq. (13), the anticrossing region is passed at time $t \approx 0$, and the frequency difference is negative for $t < 0$ and positive for $t > 0$ (see Fig. 2). With these approximations, Eq. (12) becomes

$$\ddot{c}_A - i\dot{c}_A \alpha t + c_A \Gamma^2/4 = 0. \quad (14)$$

Despite the approximations, there is no analytical solution of Eq. (14) for $c_A(t)$. However, we are not interested in the

temporal behavior of c_A but rather in the value that c_A assumes after the anticrossing regime has long passed. By using contour integration, we find that the solution for $c_A(t \rightarrow \infty)$ is¹⁵

$$c_A(\infty) = \exp \left[-\frac{\pi}{4} \Gamma^2 / \alpha \right]. \quad (15)$$

Because the energy of oscillator A is $E_A \propto |c_A|^2$, the probability for level crossing is

$$P_{\text{diab}} = \exp \left[-\frac{\pi}{2} \Gamma^2 / \alpha \right], \quad (16)$$

which is also referred to as a *diabatic transition*, a transition involving loss or gain.

Equation (16) is the classical analog of the Landau–Zener formula in quantum mechanics.^{16,17} As illustrated in Fig. 3(b), Eq. (16) defines the probability that the energy of oscillator A remains the same after transitioning through the anticrossing region. P_{diab} is the probability for passing through the anticrossing region by switching branches, that is, for jumping from one eigenmode to the other [see Fig. 3(b)]. Consequently, the probability of an adiabatic transition is $P_{\text{adiab}} = 1 - P_{\text{diab}}$.

The probability of a diabatic transition depends on the frequency splitting $\Gamma = [\omega_+ - \omega_-]$ and the time $\tau \sim \Gamma/\alpha$ that it takes to transition through the anticrossing region. A diabatic transition is likely for $\Gamma\tau \ll 1$, which corresponds to a rapid transition through the anticrossing region. In contrast, for a slow transition ($\Gamma\tau \gg 1$), an adiabatic transition is more probable. Note that the product $\Gamma\tau$ has analogies with the time-energy uncertainty principle. For times $\tau \ll 1/\Gamma$, the energy uncertainty becomes larger than the level splitting thereby “closing up” the anticrossing region and making diabatic transitions possible.

In our example, we can control which branch (eigenmode) we end up with by setting the speed at which $\Delta k(t)$ changes. Figure 4(b) shows computed results for $|c_A(t)|^2$ for two time dependences of Δk . In both cases, Δk changes from $-k_o$ to k_o , but the speed of this change is different. Figure 4(a) shows the corresponding time dependence of the frequency shifts. For the computations of c_A , we assumed that only oscillator A is active initially, that is, $c_A(-\infty) = 1$ and $c_B(-\infty) = 0$. As time evolves, we observe small oscillations in c_A and then an abrupt change in the transition region. This change is followed by a slowly damped oscillation. The two limiting values for the diabatic probability P_{diab} are indicated in Fig. 4(b). Although one of the curves represents a nearly adiabatic transition ($P_{\text{diab}} \sim 0$), the other represents a nearly diabatic transition ($P_{\text{diab}} \sim 1$). Situations in between can be selected by adjusting the speed at which $\Delta k(t)$ changes.

Let us now verify the transition probabilities using the Landau–Zener formula. A linear approximation to the curves in Fig. 4(a) yields the slopes $\alpha_1 = 0.003\omega_A^2$ and $\alpha_2 = 0.075\omega_A^2$. The level splitting of the two oscillators is $\Gamma = (\kappa/m_o)/\omega_A$, with $\omega_A^2 = (k_o + \kappa)/m_o$. If we use $\kappa = 0.08k_o$ and substitute the expressions for Γ and α into Eq. (16), we find $P_{\text{diab}}(\alpha_1) = 0.06$ and $P_{\text{diab}}(\alpha_2) = 0.89$, in agreement with the computed results in Fig. 4(b).

The accuracy of the classical Landau–Zener formula can be tested numerically for different time dependences of $\Delta k(t)$ and for different initial conditions. Students can combine the

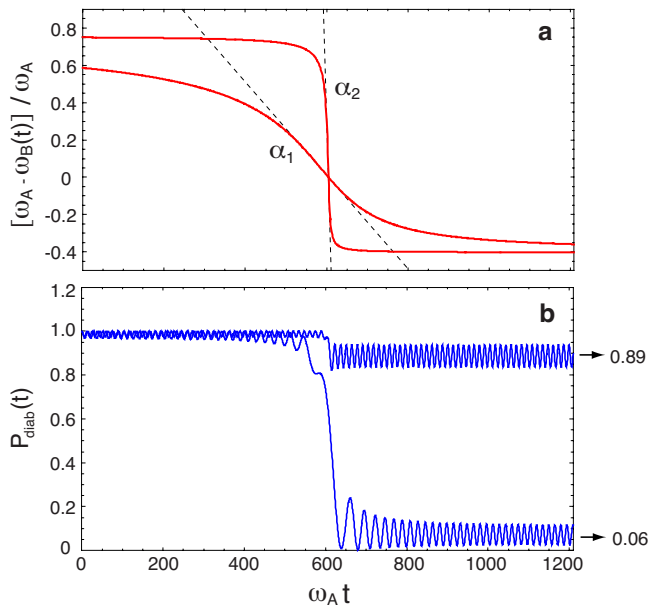


Fig. 4. Diabatic transition probability computed for two different time dependencies of $\Delta k(t)$. (a) Time dependence of the frequency shift. The linear approximation Eq. (13) yields $\alpha_1=0.003\omega_A^2$ and $\alpha_2=0.075\omega_A^2$. (b) The transition probability $P_{\text{diab}}(t)=c_A(t)c_A^*(t)$ for the two functions in (a). For a frequency difference that changes slowly (curve labeled α_1), we obtain a nearly adiabatic transition with the limiting value of $P_{\text{diab}}=0.06$, whereas a rapidly changing frequency difference (curve labeled α_2) results in a nearly diabatic transition with the limiting value of $P_{\text{diab}}=0.89$. $k_A=k_o$, $k_B=k_o+\Delta k$, $m_A=m_B=m_o$, and $\kappa=0.08k_o$.

two coupled equations in Eq. (10) to obtain two decoupled fourth-order differential equations and implement a finite difference method to follow the evolution of $c_A(t)$ and $c_B(t)$ and obtain curves similar to those shown in Fig. 4(b). To resolve all the temporal details, it is important to keep the differential time step Δt sufficiently small. The asymptotic values after transitioning through the anticrossing region can then be compared with the Landau–Zener formula.¹⁸

The Landau–Zener formula is an important result because it finds application in a wide range of problems. It allows us to readily calculate the transitions between eigenmodes of two coupled systems. The result in Eq. (16) can be extended to a quantum mechanical system with eigenstates $|1\rangle$ and $|2\rangle$ by using the substitutions $\hbar\Gamma/2 \rightarrow |\langle 1|\hat{H}_{\text{int}}|2\rangle|$ and $\hbar\alpha \rightarrow d[E_1(t)-E_2(t)]/dt$, where \hat{H}_{int} is the interaction Hamiltonian and E_i the energy eigenvalues. These substitutions yield the original quantum Landau–Zener formula.

ACKNOWLEDGMENT

The author is grateful for the financial support by the U.S. Department of Energy (Grant No. DE-FG02-01ER15204).

^{a)}Electronic mail: novotny@optics.rochester.edu

¹R. R. Chance, A. Prock, and R. Silbey, in *Molecular Fluorescence and Energy Transfer near Interfaces*, Advances in Chemical Physics, Vol. 37, edited by I. Prigogine and S. A. Rice (Wiley, New York, 1978), pp. 1–65.

²L. Novotny and B. Hecht, *Principles of Nano-Optics* (Cambridge U. P., Cambridge, 2006).

³Y. Xu, R. K. Lee, and A. Yariv, “Quantum analysis and the classical analysis of spontaneous emission in a microcavity,” *Phys. Rev. A* **61**, 033807-1–13 (2000).

⁴E. M. Purcell, “Spontaneous emission probabilities at radio frequencies,” *Phys. Rev.* **69**, 681–681 (1946).

⁵Th. Förster, “Energiewanderung und Fluoreszenz,” *Naturwiss.* **33**, 166–175 (1946); Th. Förster, “Zwischenmolekulare Energiewanderung und Fluoreszenz,” *Ann. Phys.* **2**, 55–75 (1948) An English translation of Förster’s original work is provided by R. S. Knox, “Intermolecular energy migration and fluorescence,” in *Biological Physics*, edited by E. Mielczarek, R. S. Knox, and E. Greenbaum (American Institute of Physics, New York, 1993), pp. 148–160.

⁶C. L. Garrido Alzar, M. A. G. Martinez, and P. Nussenzveig, “Classical analog of electromagnetically induced transparency,” *Am. J. Phys.* **70**, 37–41 (2002).

⁷W. Frank and P. von Brentano, “Classical analogy to quantum-mechanical level repulsion,” *Am. J. Phys.* **62**, 706–709 (1994).

⁸H. J. Maris and Q. Xiong, “Adiabatic and nonadiabatic processes in classical and quantum mechanics,” *Am. J. Phys.* **56**, 1114–1117 (1988).

⁹B. W. Shore, M. V. Gromovyy, L. P. Yatsenko, and V. I. Romanenko, “Simple mechanical analogs of rapid adiabatic passage in atomic physics,” *Am. J. Phys.* **77**, 1183–1194 (2009).

¹⁰C. Cohen-Tannoudji, J. Dupont-Roc, and G. Grynberg, *Atom-Photon Interactions* (Wiley-VCH Verlag, Weinheim, 2004), Chap. VI.

¹¹M. L. Zimmerman, M. G. Littman, M. M. Kash, and D. Kleppner, “Stark structure of the Rydberg states of alkali-metal atoms,” *Phys. Rev. A* **20**, 2251–2275 (1979).

¹²M. Bayer, P. Hawrylak, K. Hinzer, S. Fafard, M. Korkusinski, Z. R. Wasilewski, O. Stern, and A. Forchel, “Coupling and entangling of quantum dot states in quantum dot molecules,” *Science* **291**, 451–453 (2001).

¹³T. J. Kippenberg and K. J. Vahala, “Cavity optomechanics: Back-action at the mesoscale,” *Science* **321**, 1172–1176 (2008).

¹⁴A. R. Bosco de Magalhães, C. H. d’Avila Fonseca, and M. C. Nemes, “Classical and quantum coupled oscillators: Symplectic structure,” *Phys. Scr.* **74**, 472–480 (2006).

¹⁵C. Wittig, “The Landau–Zener formula,” *J. Phys. Chem. B* **109**, 8428–8430 (2005).

¹⁶L. Landau, “Zur Theorie der Energieübertragung bei Stößen II,” *Phys. Z. Sowjetunion* **2**, 46–51 (1932).

¹⁷C. Zener, “Non-adiabatic crossing of energy levels,” *Proc. R. Soc. London, Ser. A* **137**, 696–702 (1932).

¹⁸S. Geltman and N. D. Aragon, “Model study of the Landau–Zener approximation,” *Am. J. Phys.* **73**, 1050–1054 (2005).